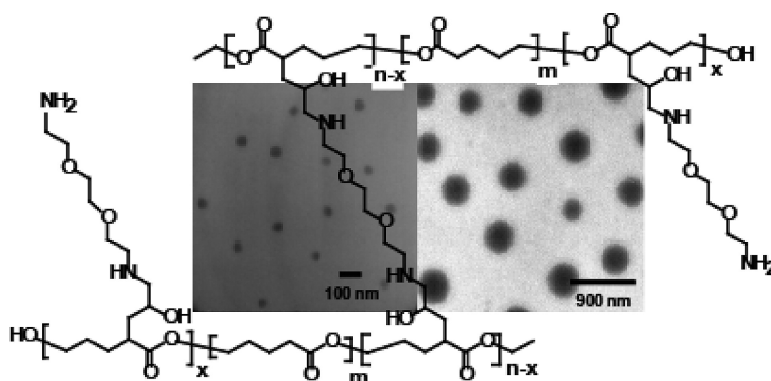


## Approach to Formation of Multifunctional Polyester Particles in Controlled Nanoscopic Dimensions

Alice E. van der Ende, Evan J. Kravitz, and Eva Harth

*J. Am. Chem. Soc.*, **2008**, 130 (27), 8706-8713 • DOI: 10.1021/ja7111417h • Publication Date (Web): 11 June 2008

Downloaded from <http://pubs.acs.org> on February 8, 2009



### More About This Article

Additional resources and features associated with this article are available within the HTML version:

- Supporting Information
- Access to high resolution figures
- Links to articles and content related to this article
- Copyright permission to reproduce figures and/or text from this article

[View the Full Text HTML](#)

### Approach to Formation of Multifunctional Polyester Particles in Controlled Nanoscopic Dimensions

Alice E. van der Ende, Evan J. Kravitz, and Eva Harth\*

Department of Chemistry and Pharmacology, Vanderbilt University, 7619 Stevenson Center, Nashville, Tennessee 37235

Received December 26, 2007; Revised Manuscript Received April 16, 2008; E-mail: eva.harth@vanderbilt.edu

**Abstract:** We present the synthesis of discrete functionalized polyester nanoparticles in selected nanoscale size dimensions via a controlled intermolecular chain cross-linking process. The novel technique involves the controlled coupling of epoxide functionalized polyesters with 2,2'-(ethylenedioxy)bis(ethylamine) to give well-defined nanoparticles with narrow size distribution and selected nanoscopic size dimensions. Diverse functionalized polyesters, synthesized with pendant functionalities via ring-opening copolymerization of  $\delta$ -valerolactone with  $\alpha$ -allyl- $\delta$ -valerolactone,  $\alpha$ -propargyl- $\delta$ -valerolactone and 2-oxepane-1,5-dione, were prepared as linear precursors which facilitated 3-D nanoparticles with functionalities such as amines, keto groups, and alkynes for post modification reactions. We found that the nanoparticle formation and the control over the nanoscopic dimension is primarily influenced by the degree of the epoxide entity implemented in the precursor polymers and the amount of 2,2'-(ethylenedioxy)bis(ethylamine) as cross-linking reagent. The other functionalities in the linear polyester do not participate in the nanoparticle formation and particles with defined functionalities can be prepared from batches of identical linear polymers containing various functionalities or by mixing different polyester materials to achieve controlled amounts of specific functional groups. The utilization of integrated functionalities was demonstrated in one post-modification reaction with *N*-Boc-ethylenediamine via reductive amination. This work describes the development of a novel methodology to prepare functionalized well-defined 3-D nanoparticle polyester materials in targeted nanoscopic ranges with amorphous morphologies or tailored crystallinities that offer a multitude of utilizations as a result of their unique properties and control in preparation.

#### Introduction

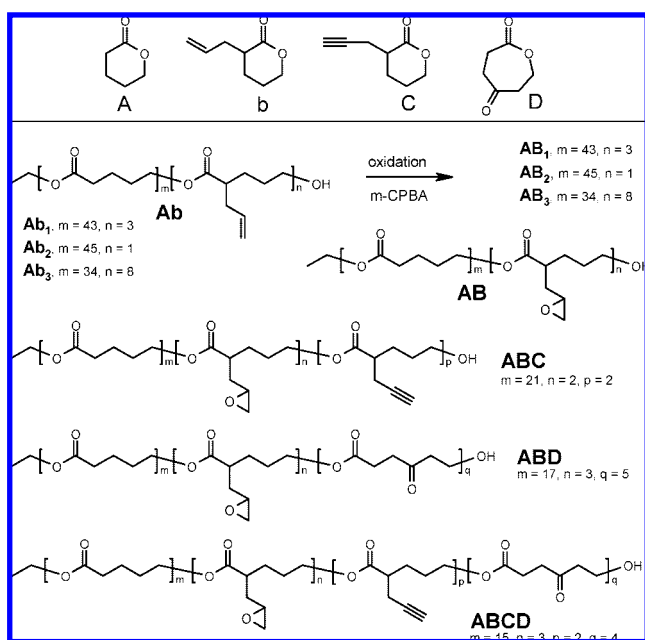
Degradable aliphatic polyester materials, such as poly(L-lactic acid) (PLLA), poly(glycolic acid) (PGA), poly( $\epsilon$ -caprolactone) (PCL), and their copolymers, have received considerable attention in the medical and pharmaceutical fields, finding applications as drug delivery systems,<sup>1</sup> implant materials,<sup>2</sup> and diagnostic systems.<sup>3</sup> In many of these applications, in particular for drug delivery purposes, the polyester materials are administered in the form of nanoparticles, as they are able to cross physiological epithelial barriers and give means to controlled

release profiles. However, the majority of these polyesters are restricted in their utility, due to their crystalline and hydrophobic properties,<sup>4</sup> which influence their physicochemical properties, together with challenges to provide particles in well-defined sizes and well-characterized surface properties.<sup>5</sup> The control over particle sizes has been recognized to be crucial to predict the interaction with cells and other biological barriers,<sup>6</sup> but discrepancies in size distributions and shape, caused by the lack of reproducibility of common methodologies, have led to difficulties in interpreting and controlling biological responses. Current techniques are profoundly influenced by the selection

\* To whom correspondence should be addressed.

- (1) (a) Alexis, F.; Rhee, J. W.; Richie, J. P.; Radovic-Moreno, A. F.; Langer, R.; Farokhzad, O. C. *Urol. Oncol.-Semin. Ori.* **2008**, *26*, 74–85. (b) Uhrich, K. E.; Cannizzaro, S. M.; Langer, R. S.; Shakesheff, K. M. *Chem. Rev.* **1999**, *99*, 3181–3198. (c) Shuai, X. T.; Ai, H.; Nasongkla, N.; Kim, S.; Gao, J. M. *J. Controlled Release* **2004**, *98*, 415–426. (d) Langer, R. *Acc. Chem. Res.* **2000**, *33*, 94–101. (e) Kohane, D. S.; Tse, J. Y.; Yeo, Y.; Padera, R.; Shubina, M.; Langer, R. *J. Biomed. Mater. Res. A* **2006**, *77A*, 351–361. (f) Cheng, J.; Teply, B. A.; Sherifi, I.; Sung, J.; Luther, G.; Gu, F. X.; Levy-Nissenbaum, E.; Radovic-Moreno, A. F.; Langer, R.; Farokhzad, O. C. *Biomaterials* **2007**, *28*, 869–876.
- (2) (a) Agrawal, C. M.; Haas, K. F.; Leopold, D. A.; Clark, H. G. *Biomaterials* **1992**, *13*, 176–182. (b) Nuutinen, J.-P.; Valimaa, T.; Clerc, C.; Tormala, P. *J. Biomater. Sci., Polym. Ed.* **2002**, *13*, 1313–1323. (c) Valimaa, T.; Laaksovirta, S.; Tammela, T. L. J.; Laippala, P.; Talja, M.; Isotalo, T.; Petas, A.; Tarri, K.; Tormala, P. *Biomaterials* **2002**, *23*, 3575–3582. (d) Tomita, M.; Lavik, E.; Klassen, H.; Zahir, T.; Langer, R.; Young, M. *J. Stem Cells* **2005**, *23*, 1579–1588. (e) Wuisman, P. I. J. M.; Smit, T. H. *Eur. Spine J* **2006**, *15*, 133–148. (f) Yang, J.; Webb, A. R.; Ameer, G. A. *Adv. Mater.* **2004**, *16*, 511.

- (3) (a) Nasongkla, N.; Bey, E.; Ren, J. M.; Ai, H.; Khemtong, C.; Guthi, J. S.; Chin, S. F.; Sherry, A. D.; Boothman, D. A.; Gao, J. M. *Nano. Lett.* **2006**, *6*, 2427–2430. (b) Mouffouk, F.; Chishtii, Y.; Jin, Q. L.; Rosa, M. E.; Rivera, M.; Dasa, S.; Chen, L. H. *Anal. Biochem.* **2008**, *372*, 140–147. (c) Park Yoon, J.; Lee Jue, Y.; Chang Young, S.; Jeong Jae, M.; Chung Jun, K.; Lee Myung, C.; Park Kyoung, B.; Lee Seung, J. *Biomaterials* **2002**, *23*, 873–879.
- (4) (a) Zhang, Z. P.; Feng, S. S. *Biomaterials* **2006**, *27*, 262–270. (b) Olson, D. A.; Gratton, S. E. A.; DeSimone, J. M.; Sheares, V. V. *J. Am. Chem. Soc.* **2006**, *128*, 13625–13633. (c) Olson, D. A.; Sheares, V. V. *Macromolecules* **2006**, *39*, 2808–2814.
- (5) Delie, F. *Adv. Drug Delivery Rev.* **1998**, *34*, 221–233.
- (6) (a) Maassen, S.; Fattal, E.; Mueller, R. H.; Couvreur, P. *S.T.P. Pharma Sci.* **1993**, *3*, 11–22. (b) Dong, Y. C.; Feng, S. S. *Biomaterials* **2005**, *26*, 6068–6076. (c) Win, K. Y.; Feng, S. S. *Biomaterials* **2005**, *26*, 2713–2722. (d) Durrer, C.; Irache, J. M.; Duchene, D.; Ponchel, G. *Prog. Colloid Polym. Sci.* **1994**, *97*, 275–80. (e) Jani, P.; Halbert, G. W.; Langridge, J.; Florence, A. T. *J. Pharm. Pharmacol.* **1990**, *42*, 821–6.

**Table 1.** Multifunctional Linear Polyester Precursors with Epoxide Cross-Linking Moieties

of the stabilizer and solvent and, therefore, are limited to only a range of specific nanoparticle size dimensions. For example, solvent displacement,<sup>7</sup> emulsion-diffusion-evaporation,<sup>8</sup> and salting-out methods<sup>9</sup> usually produce particles with size dimensions greater than 100 nm, whereas other approaches utilizing nonaqueous emulsion polymerization lead to polyester nanoparticle size from 38–60 nm.<sup>10</sup> In the effort to achieve the necessary narrow nanoparticle dispersities, many of these methods require centrifugation steps to yield particles with size standard deviations that do not exceed 20%.<sup>11</sup> In these purification steps, not only particles, but also drug molecules that are typically encapsulated during nanoparticle formation are lost. Furthermore, a low drug load during nanoparticle formation is required (1–5%) to prevent high polydispersities of the resulting particles.<sup>1f</sup> An ideal methodology, however, would provide a practical formation of functionalized monodisperse, amorphous particles with a variety of distinct size dimensions and would address the aforementioned challenges.

In addition to the demand for well-defined nanoparticles with control over size and a wide range of different nanoparticle dimensions, hydrophilicity and the integration of functionalities will be key factors to utilize polyester materials in the increasingly specified applications of the biomedical arena. Recent

reports have described efforts to predict and increase the mechanical and degradation properties by reacting diols with diacids to create poly(ester ether) via polycondensation reactions.<sup>4c</sup> Other approaches have attached short polyethylene glycol units onto functional groups in linear polyesters prepared from  $\delta$ -valerolactones in ring-opening polymerization procedures.<sup>4a</sup> These examples document that the amorphous nature or limited crystallinity can greatly improve the property control and tailor the material toward individual biological environments.<sup>4,12</sup> In this vein, a variety of new lactone polymerization catalysts<sup>13</sup> have accelerated the investigations of ring-opening polymerizations involving substituted lactones that have proven to be a valuable asset to introduce pendant functionalities along the linear polyester backbones. Monomers, such as  $\delta$ -valerolactone and  $\alpha$ -propargyl- $\delta$ -valerolactone, have been copolymerized and investigated in post-modification strategies<sup>14</sup> to form bioconjugates containing peptidic targeting units and other bioactive compounds utilizing the integrated pendant functionality.<sup>15</sup> Traditional aliphatic polyesters, however, suffer from the lack of functional groups<sup>16</sup> and those precedent developments support the efforts to foster properties that tune polyesters into refined polymers with sites that influence hydrophilicity, biorecognition, and bioadhesion.<sup>17</sup>

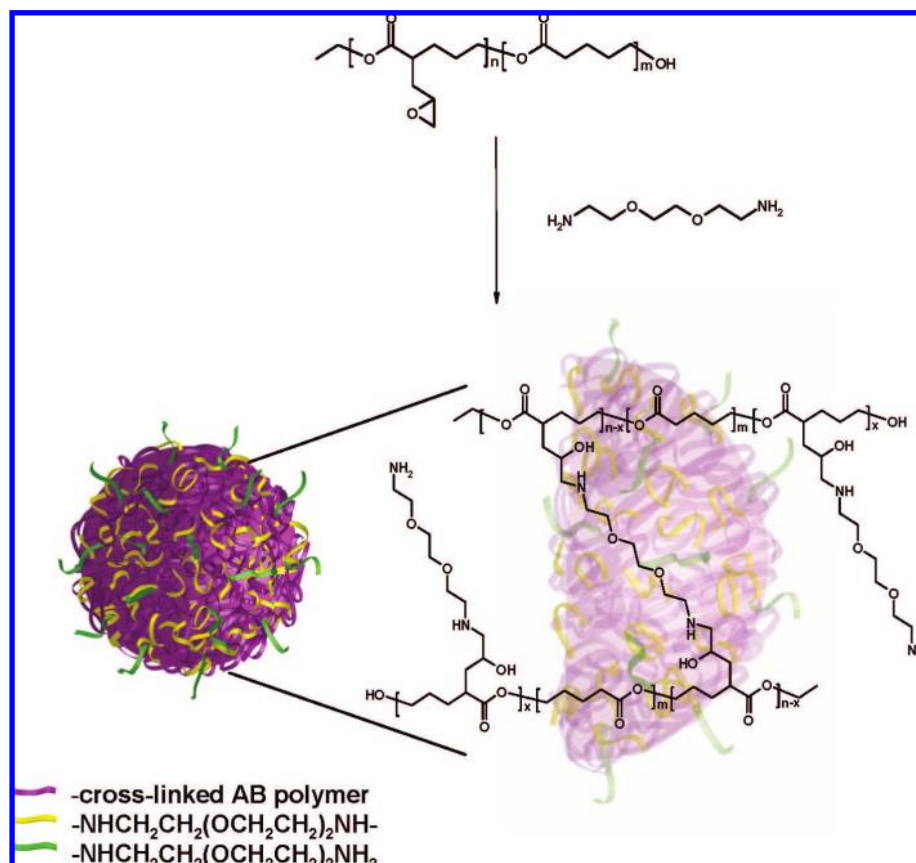
This work describes a practical strategy for the formation of polyester particles with amorphous and semicrystalline morphologies in a variety of distinct nanoscopic ranges through a controlled cross-linking strategy that allows the formation of 3-D polyester architectures that not only inherit the solubility of their linear polymer precursors, but also contain a variety of functionalities as a result of the cross-linking process with one type of linear polyester or a mixture of different linear chains. The presented technique bears opportunities that will further advance the application potential of polyester based materials in the biomedical field.

## Results and Discussion

In our strategy, we were drawn to investigate controlled cross-linking methods for generating functionalized and amorphous nanoparticles, rather than employing salting-out strategies,<sup>9</sup> solvent displacement techniques,<sup>7</sup> emulsion polymerization,<sup>10,18</sup> or emulsion diffusion methods<sup>8</sup> that require salts or surfactants,

- (7) (a) Renard, E.; Ternat, C.; Langlois, V.; Guerin, P. *Macromol. Biosci.* **2003**, *3*, 248–252. (b) Oster, C. G.; Wittmar, M.; Bakowsky, U.; Kissel, T. *J. Controlled Release* **2006**, *111*, 371–381. (c) Chawala, J. S.; Amiji, M. M. *Int. J. Pharm.* **2002**, *249*, 127–138.
- (8) (a) Kumar, M. N. V. R.; Bakowsky, U.; Lehr, C. M. *Biomaterials* **2004**, *25*, 1771–1777. (b) Kumar, M. N. V. R.; Mohapatra, S. S.; Kong, X.; Jena, P. K. I.; Bakowsky, U.; Lehr, C. M. *J. Nanosci. Nanotechnol.* **2004**, *4*, 990–994.
- (9) (a) Zweers, M. L. T.; Grijpma, D. W.; Engbers, G. H. M.; Feijen, J. *J. Biomed. Mater. Res., Part B: Appl. Biomater.* **2003**, *66B*, 559–566. (b) Konan, Y. N.; Gurny, R.; Allemann, E. *Int. J. Pharm.* **2002**, *233*, 239–252. (c) Galindo-Rodriguez, S.; Allemann, E.; Fessi, H.; Doelker, E. *Pharm. Res.* **2004**, *21*, 1428–1439. (d) Zweers, M. L. T.; Engbers, G. H. M.; Grijpma, D. W.; Feijen, J. *J. Controlled Release* **2006**, *114*, 317–324.
- (10) Muller, K.; Klapper, M.; Mullen, K. *J. Polym. Sci. Part A: Polym. Chem.* **2007**, *45*, 1101–1108.
- (11) Gaumet, M.; Gurny, R.; Delie, F. *Int. J. Pharm.* **2007**, *342*, 222–230.

- (12) (a) Amsden, B. G.; Misra, G.; Gu, F.; Younes, H. M. *Biomacromolecules* **2004**, *5*, 2479–2486. (b) Brown, A. H.; Sheares, V. V. *Macromolecules* **2007**, *40*, 4848–4853.
- (13) (a) Cordova, A.; Hult, A.; Hult, K.; Ihre, H.; Iversen, T.; Malmstrom, E. *J. Am. Chem. Soc.* **1998**, *120*, 13521–13522. (b) Kricheldorf, H. R.; Lee, S. R.; Bush, S. *Macromolecules* **1996**, *29*, 1375–1381. (c) Pang, X.; Chen, X.; Zhuang, X.; Jing, X. *J. Polym. Sci., Part A: Polym. Chem.* **2007**, *46*, 643–649. (d) Cobb, A. J. A.; Marson, C. M. *Tetrahedron* **2005**, *61*, 1269–1279. (e) Coulembier, O.; Delcourt, C.; Dubois, P. *Open Macromol. J* **2007**, *1*, 1–5. (f) Douglas, A. F.; Patrick, B. O.; Mehrkhodavandi, P. *Angew. Chem., Int. Ed.* **2008**, *47*, 2290–2293. (g) Kowalski, A.; Duda, A.; Penczek, S. *Macromolecules* **2000**, *33*, 7359–7370. (h) Kowalski, A.; Libiszowski, J.; Biela, T.; Cypryk, M.; Duda, A.; Penczek, S. *Macromolecules* **2005**, *38*, 8170–8176.
- (14) Van Horn, B. A.; Iha, R. K.; Wooley, K. L. *Macromolecules* **2008**, *41*, 1618–1626.
- (15) Parrish, B.; Emrick, T. *Macromolecules* **2004**, *37*, 5863–5865.
- (16) (a) Sasatsu, M.; Onishi, H.; Machida, Y. *Int. J. Pharm.* **2006**, *317*, 167–174. (b) Mohamed, F.; van der Walle, C. F. *J. Pharm. Sci.* **2008**, *97*, 71–87.
- (17) (a) Riva, R.; Lenoir, S.; Jerome, R.; Lecomte, P. *Polymer* **2005**, *46*, 8511–8518. (b) Parrish, B.; Breitenkamp, R. B.; Emrick, T. *J. Am. Chem. Soc.* **2005**, *127*, 7404–7410. (c) Galindo-Rodriguez, S.; Allemann, E.; Fessi, H.; Doelker, E. *Pharm. Res.* **2004**, *21*, 1428–1439.
- (18) Taden, A.; Antonietti, M.; Landfester, K. *Macromol. Rapid Commun.* **2003**, *24*, 512–516.

**Scheme 1.** Nanoparticle Formation by Covalent Crosslinking with 2,2'-(Ethylenedioxy)bis(ethylamine)

which are difficult to remove sufficiently after particle formation.<sup>19</sup> It was found that reacting epoxide groups with diamines to form alkane-OH groups could provide clean and nontoxic cross-linking. While this cross-linking technique has been employed to form acrylate-based microparticles<sup>20</sup> and hydrogels,<sup>21</sup> it has never been investigated in the formation of degradable nanoparticles, due to the lack of suitable linear precursors. Therefore, we proceeded to integrate the epoxide entity, for the formation of discrete cross-linked nanoparticles, first by polymerization of a low molecular weight linear copolymer, **Ab**<sub>1</sub>, with pendant allyl groups. Pendant allyl groups represent valuable intermediates to many functional groups and, therefore, were incorporated into the polymer backbone by copolymerizing  $\alpha$ -allyl- $\delta$ -valerolactone, (b), and commercially available  $\delta$ -valerolactone, (A), via ring-opening polymerization (ROP), as reported.<sup>22</sup> Upon copolymerization, the pendant allyl groups of **Ab**<sub>1</sub> were oxidized with meta-chloroperoxybenzoic acid (*m*-CPBA)<sup>23</sup> under mild conditions to convert the double bonds to epoxide rings to give **AB**<sub>1</sub> (Table 1) that contained, thereby, the crucial functionality in nanoparticle formation via controlled cross-linking. In order to introduce various functionalities into the resulting particles, additional monomers were synthesized,

$\alpha$ -propargyl- $\delta$ -valerolactone, (C),<sup>17b</sup> and 2-oxepane-1,5-dione, (D),<sup>24</sup> according to the literature. These monomers were then individually copolymerized with (b) and  $\delta$ -valerolactone, (A), in a similar manner as **Ab**<sub>1</sub>, to give rise to novel polyesters with acetylene or keto functionalities, respectively. In addition to these copolymers, polymer **AbCD** was synthesized, which further increased the number of functional groups. These functionalities are anticipated to enrich the nanoparticle utilization and to govern orthogonal conjugation strategies for targeting units, dyes, and a dendritic molecular transporter.<sup>25</sup> After polymerizing each of the aforementioned copolymers, the formation of the epoxide groups was achieved by oxidizing the pendant allyl functionalities with *m*-CPBA (Table 1). The modified copolymers were obtained in molecular weight ranges of 3400–4800 Da with narrow polydispersities of 1.16–1.27.

The formation of nanoparticles in controlled size dimensions progressed from covalently cross-linking the epoxide functionalized linear polymers with 2,2'-(ethylenedioxy)bis(ethylamine) (Scheme 1). In order to study the particle formation under controlled conditions, we first performed various experiments with linear polymer **AB**<sub>1</sub>, in which a solution of **AB**<sub>1</sub> in dichloromethane of known concentration was added dropwise (13 mL/min) to a refluxing solution of 2,2'-(ethylenedioxy)bis(ethylamine) in dichloromethane. We chose specifically 2,2'-(ethylenedioxy)bis(ethylamine), as the diamine cross-linking reagent, to enhance the hydrophilic, and amorphous properties of the resulting particle. In the first set of experiments, polymer

(19) Kallinteri, P.; Higgins, S.; Hutcheon, G. A.; St. Pourcain, C. B.; Garnett, M. C. *Biomacromolecules* **2005**, *6*, 1885–1894.

(20) Burke, S. K.; Slatopolsky, E. A.; Goldberg, D. I. *Nephrol. Dial. Transplant.* **1997**, *12*, 1640–1644.

(21) Kioussis, D. R.; Smith, D. F.; Kofinas, P. *J. Appl. Polym. Sci.* **2001**, *80*, 2073–2083.

(22) Parrish, B.; Quansah, J. K.; Emrick, T. J. *Polym. Sci., Part A: Polym. Chem.* **2002**, *40*, 1983–1990.

(23) Mecerreyes, D.; Miller, R. D.; Hedrick, J. L.; Detrembleur, C.; Jerome, R. *J. Polym. Sci., Part A: Polym. Chem.* **2000**, *38*, 870–875.

(24) Latere, J.-P.; Lecomte, P.; Dubois, P.; Jerome, R. *Macromolecules* **2002**, *35*, 7857–7859.

(25) Huang, K.; Voss, B.; Kumar, D.; Hamm, H. E.; Harth, E. *Bioconjugate Chem.* **2007**, *18*, 403–409.



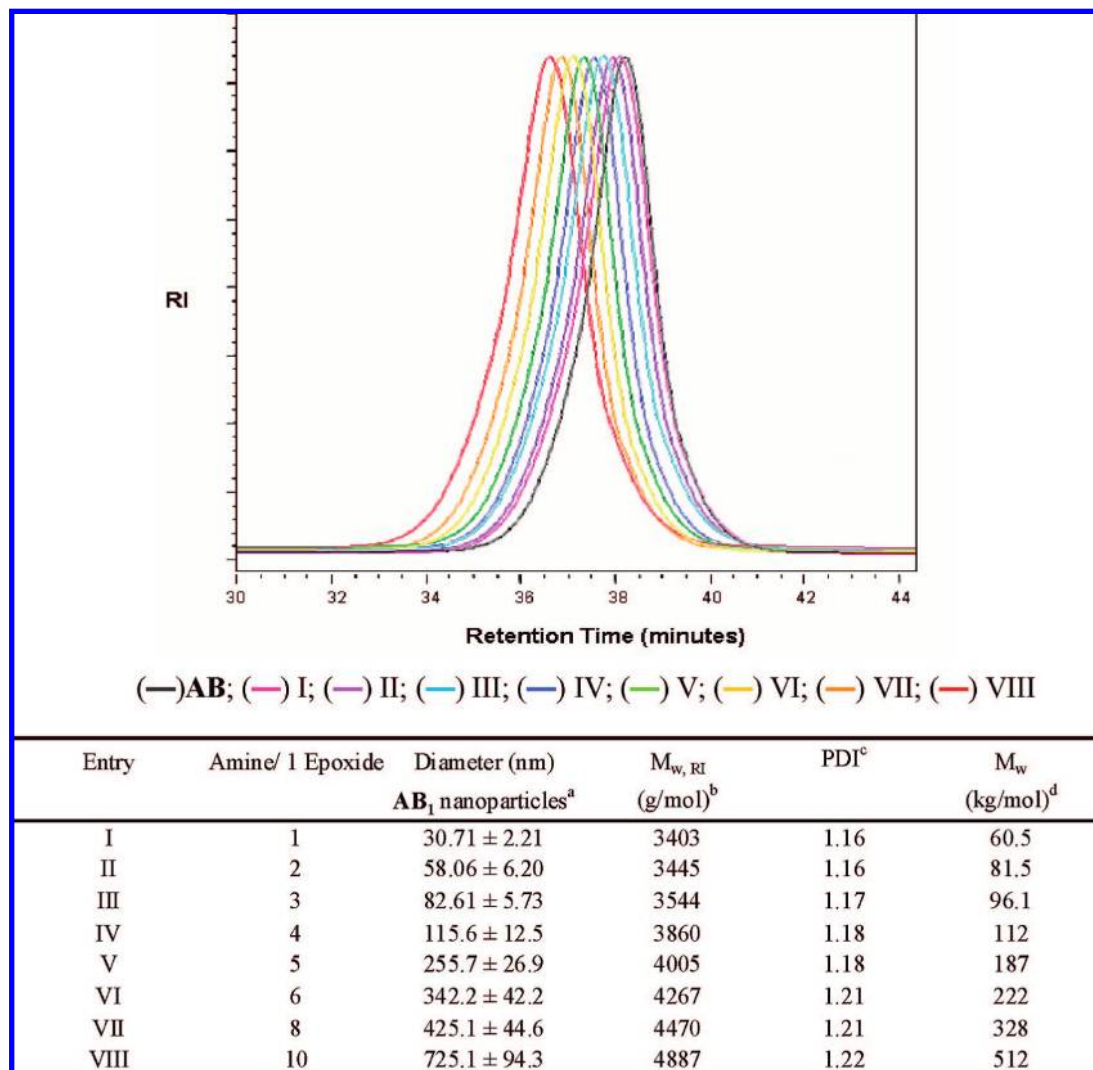


**Figure 1.** (a,top) Overlay of GPC traces for **AB** the linear polyester precursor,  $M_w = 3403$ ,  $PDI = 1.16$ ; and nanoparticles **AB<sub>1</sub>** (I–VIII) derived from controlled cross-linking with increasing equivalents (1–10) of amine per epoxide group; (b, bottom) <sup>a</sup>hydrodynamic diameter of **AB<sub>1</sub>** nanoparticle series measured by dynamic light scattering (DLS), <sup>b</sup>gel permeation chromatography (GPC) data of the cross-linked nanoparticle **AB<sub>1</sub>** series relative to PS standards; weight-average molecular weight ( $M_w$ ) after dialysis; and <sup>c</sup>polydispersity ( $PDI = M_w/M_n$ ), measured by GPC with tetrahydrofuran as eluent and integrated RI detector; <sup>d</sup>weight-average molecular weight, measured by static light scattering (SLS).

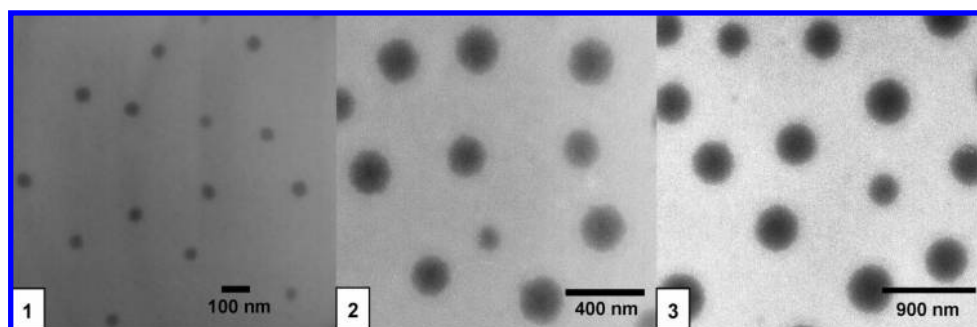


**Figure 2.** TEM images of **AB<sub>1</sub>** nanoparticles: (1) 2 equiv. of amine; (2) 5 equiv. of amine, and (3) 8 equiv. of amine.

solutions with concentrations varying from 0.1 to 0.7 M were prepared and each was dropped into its respective refluxing solution of dichloromethane containing 1 or 2 equiv. of amine per pendant epoxide cross-linking entity being added. While each of these reactions was successful in producing small quantities of nanoparticles after refluxing for 4 h, as evidenced by dynamic light scattering (DLS), there was still a considerable

amount of remnant starting **AB<sub>1</sub>** polymer. Therefore, in order to drive the cross-linking to completion, the refluxing time was increased from 4 to 12 h, which significantly improved the yield of nanoparticles. It was observed that during particle formation, the linear precursor and the formed particles are both soluble in dichloromethane, and the reaction mixture remains clear for the duration of the cross-linking reaction. Because of the low

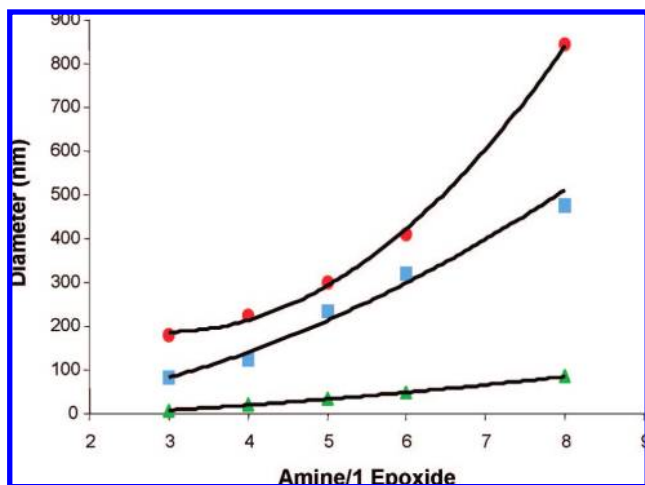


**Figure 3.** Variation in nanoparticle sizes for differing percents of oxirane in the starting linear **AB**: (▲) **AB**<sub>2</sub> nanoparticles with 2% epoxy groups; (■) **AB**<sub>1</sub> nanoparticles with 7% epoxy groups, and; (●) **AB**<sub>3</sub> nanoparticles with 19% epoxy groups.

**Table 2.** Nanoparticle Size Dimensions for **AB** Particles with Varying Percentages of Epoxide Groups

amine/1 epoxide	diameter (nm) <b>AB</b> <sub>2</sub> nanoparticles 2% epoxide	diameter (nm) <b>AB</b> <sub>1</sub> nanoparticles 7% epoxide	diameter (nm) <b>AB</b> <sub>3</sub> nanoparticles 19% epoxide
3	8.0 ± 0.6	82.6 ± 5.7	179.9 ± 18.0
4	19.0 ± 1.3	115.6 ± 12.5	225.6 ± 22.5
5	33.6 ± 1.9	255.7 ± 26.9	299.0 ± 31.2
6	48.7 ± 3.2	342.2 ± 42.2	409.1 ± 42.7
8	84.9 ± 10.5	425.1 ± 44.6	843.3 ± 88.0

cross-linking density, the nanoparticle retains the physicochemical behavior of the linear polymer precursor as it was also observed in nanoparticle structures from intramolecular chain collapse processes introduced by Hawker and co-workers.<sup>26</sup>

With the goal to form monodisperse particles with controlled nanoscopic size dimensions, we investigated the effect of varying the amount of diamine available for cross-linking in a second series of experiments. The equivalents of diamine cross-linker were increased from 1 to 10 amines per epoxide group in **AB**<sub>1</sub> while using a polymer solution of 0.5 M, which were found to be the optimal conditions to observe distinguishable changes in particle sizes. The precision of nanoparticle formation was examined in detail using the resulting **AB**<sub>1</sub> particles, and it was shown that the controlled cross-linking is a facile process that gives well-defined nanoparticles with a polynomial increase in molecular weight and hydrodynamic diameter. As can be seen in Figure 1, the GPC traces shift to higher hydrodynamic diameters with systematically increasing equivalents of diamine cross-linker per epoxide groups of the linear precursor chain. One of the pertinent features of the GPC traces is their symmetrical nature accompanied by narrow polydispersities and the lack of any high molecular-weight shoulders. In each case, the nanoparticles show lower molecular weights, and the actual molecular weight is determined with static light scattering. For example, the **AB**<sub>1</sub> linear polymer with the initial  $M_w$  of 3400 Da, when reacted with 4 equiv. of amine per epoxide, gives a particle with the molecular weight of 3860 Da

and a polydispersity of 1.18. However, the actual molecular weight of this particle was found to be 112 000 Da by static light scattering, which demonstrates that there is a significant increase in molecular weight during the cross-linking process, but with no significant increase of the polydispersity as compared to the starting material. The unique feature of being able to accurately control the nanoparticle sizes is also apparent through dynamic light scattering measurements (DLS) which shows a polynomial increase in nanoscopic diameter (Figures 1 and 7, see also Supporting Information) with only 10% standard deviation that improves the typical 20% standard deviation accepted for particles derived from well-defined linear precursors for example through micellization or standard techniques that provides polyester particles after centrifugation.<sup>11</sup> Transmission electron microscopy (TEM) images from three selected particles of the **AB**<sub>1</sub> series, shown in Figure 2, underline the versatility of the novel approach to prepare spherical nanoparticles in narrow nanoscopic size dimensions, controlled by the equivalents of diamine.

The ability to control the size of the nanoparticles was examined in further detail using three different linear **AB** polymers with varying levels of epoxide incorporation: 2% **AB**<sub>2</sub>, 7% **AB**<sub>1</sub>, and 19% **AB**<sub>3</sub>. We found that the conversion of the **AB** series into nanoparticles is a facile process at all percentages of epoxide units studied. For example, we could obtain particles in sizes of 85 nm for eight amines per epoxide, whereas five amines per epoxide were necessary to achieve a 33 nm size dimension. Comparable values were obtained with 3 and 1 equiv. of amine in polymers containing 7% epoxide as with the **AB**<sub>1</sub> nanoparticle series (Table 2 and Figure 1, b bottom) demonstrated. We can conclude a systematic increase in the nanoparticle size dimensions was also observed with the increase of the epoxide groups in linear precursor polymers, which is consistent with a rise in the level of intermolecular chain coupling in the presence of increased amounts of diamine cross-linker (Figure 3).

Further characterization of the particles with <sup>1</sup>H NMR also confirmed nanoparticle formation since the diamine's methylene protons adjacent to the amine functionalities experience a shift in resonance from 2.86 to 2.89 ppm due to the transformation of the primary amine to the secondary amine after successful cross-linking with the polymer. In addition, <sup>1</sup>H NMR was able to indicate an increase in particle size, since the signals at 3.63, 3.54, and 2.89 ppm corresponding to the methylene protons neighboring the secondary amines of the ethylene dioxide linker intensified as the particles became larger in size (Figure 4).

Important information regarding the morphology of the nanoparticles was inferred from their thermal properties gathered through differential scanning calorimetry (DSC). Several **AB**<sub>1</sub> nanoparticle samples, 30.7 ± 2.2 nm, 115.6 ± 12.5 nm, and 725.1 ± 94.3 nm were analyzed by DSC to learn how the increased ratios of 2,2'-(ethylenedioxy)bis(ethylamine) accompanied by the increased nanoscopic size affected the melting transitions of the particles (Figure 5). In comparison, we investigated also particles that were formed from the **AB**<sub>2</sub> and **AB**<sub>3</sub> series in order to evaluate the influence of lower (2%) and higher (19%) percentages of epoxides incorporated into the linear precursor chains which led to lower and higher cross-linking densities of the respective nanoparticles. The nanoparticles from the **AB**<sub>1</sub> series are totally amorphous at the intended temperature of use, at 37 °C, with glass transition temperatures reaching from -25.4 to -33.2 °C. In this series, the crystallinity ranged from 19.9% to 21.3%, with the highest value being for

(26) Harth, E.; Van Horn, B.; Lee, V. Y.; Germack, D. S.; Gonzales, C. P.; Miller, R. D.; Hawker, C. J. *J. Am. Chem. Soc.* **2002**, *124*, 8653–8660.

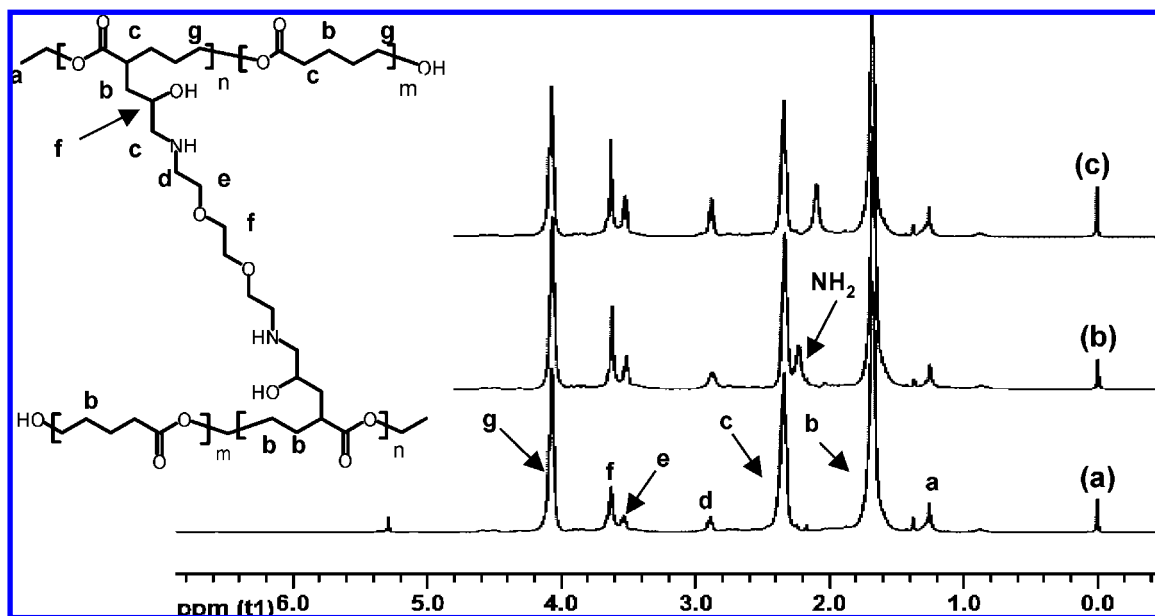


**Figure 4.**  $^1\text{H}$  NMR spectra (300 MHz,  $\text{CDCl}_3/\text{TMS}$ ) of  $\text{AB}_1$  nanoparticles with increasing cross-linking: (a) 6 amines/1 epoxide; (b) 8 amines/1 epoxide, and; (c) 10 amines/1 epoxide. The chemical structure of the cross-linked particle and appropriate proton resonance assignments are shown.

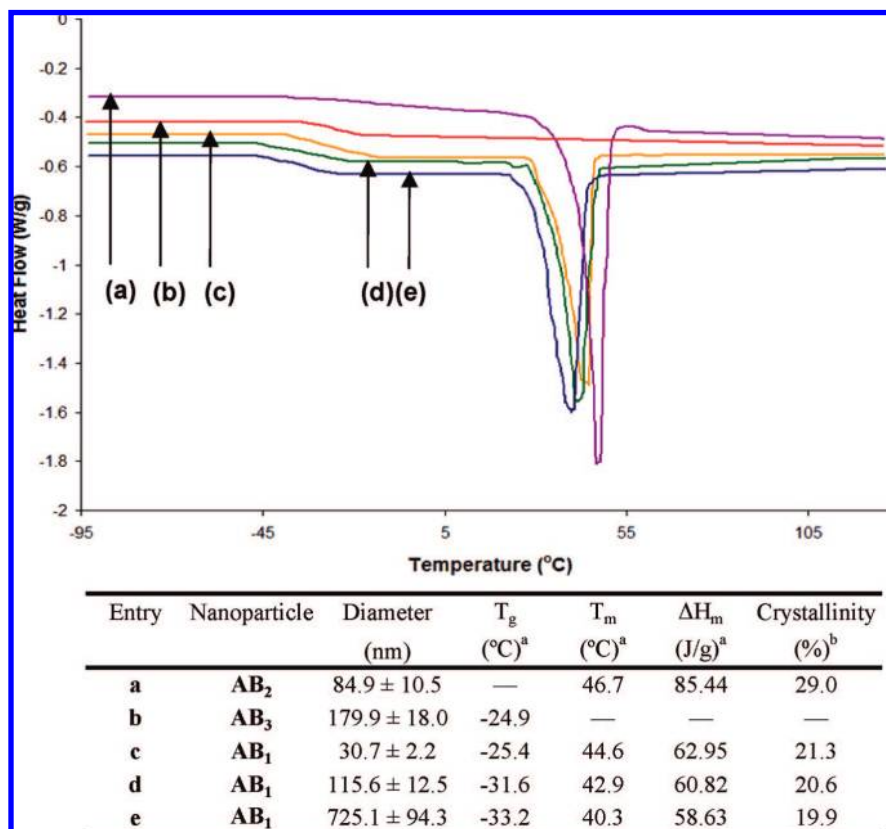


**Figure 5.** DSC trace overlay of  $84.89 \pm 10.47$  nm  $\text{AB}_2$  nanoparticles (a),  $179.9 \pm 18.0$  nm  $\text{AB}_3$  nanoparticles (b), and  $30.7 \pm 2.2$  nm  $\text{AB}_1$  nanoparticles (c),  $115 \pm 12.5$  nm  $\text{AB}_1$  nanoparticles (d), and  $725.1 \pm 94.3$  nm  $\text{AB}_1$  nanoparticles (e) in the glass and melting transition regions. <sup>a</sup>Determined by DSC. <sup>b</sup>Determined by taking the ratios of  $\Delta H_m$  of the samples to the  $\Delta H_m$  of a 100% crystalline polyester.

the smallest particle,  $30.7 \pm 2.2$  nm. As the crystallinity decreases with increasing diameter of the nanoparticle, we observe a shift of the melting temperature from 44.6 to 40.3  $^{\circ}\text{C}$ . In comparison, the nanoparticle from the  $\text{AB}_2$  series showed an expected higher crystallinity of 29% that lead to a higher melting temperature, which is in agreement with the trend observed for the  $\text{AB}_1$  series as a result of the lower density of

cross-linking units in the linear precursor chain (2%) that led to fewer cross-linking events. At higher densities of cross-linking, as experienced with higher percentages of epoxide groups along the linear precursor backbone (19%), the resulting particle from the  $\text{AB}_3$  series is totally amorphous since a glass transition temperature, at  $-24.9$   $^{\circ}\text{C}$ , and no melting transition, was observed. Therefore, we can conclude that the particles can

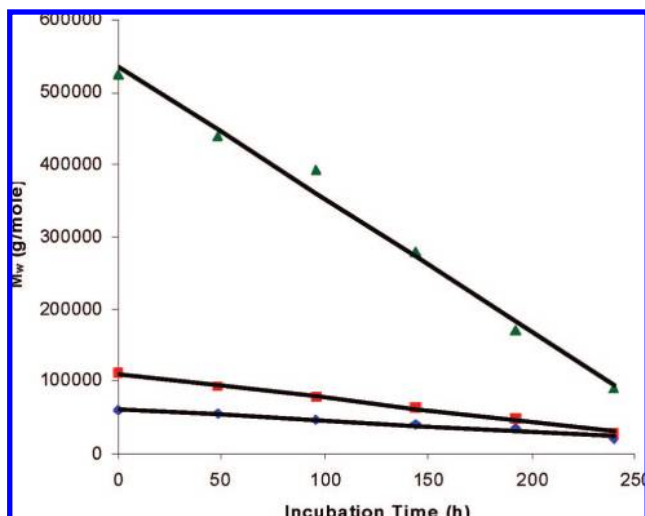


**Figure 6.** Hydrolytic degradation studies of ( $\blacktriangle$ )  $725.1 \pm 94.3$  nm  $AB_1$  nanoparticles; ( $\blacksquare$ )  $115.6 \pm 12.5$  nm  $AB_1$  nanoparticles; and ( $\blacklozenge$ )  $30.71 \pm 2.21$  nm  $AB_1$  nanoparticles.

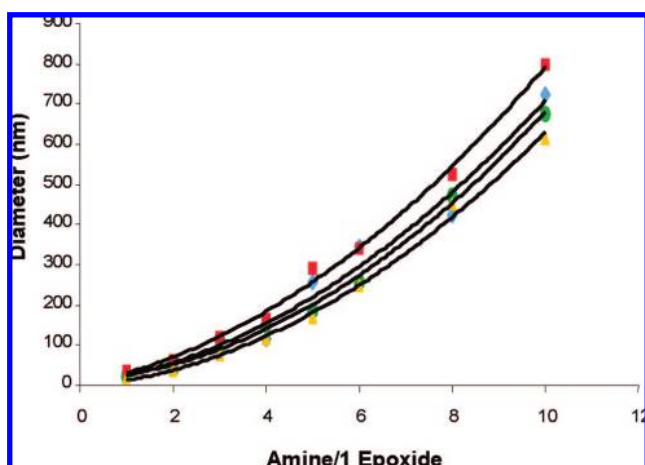


**Figure 7.** Polynomial increase in nanoparticle size with increasing equivalents of amine cross-linker: ( $\blacksquare$ ) ABD nanoparticles; ( $\blacklozenge$ )  $AB_1$  nanoparticles; ( $\bullet$ ) ABC nanoparticles; and ( $\blacktriangle$ ) ABCD nanoparticles.

be tuned to give either totally amorphous particles or particles with amorphous behavior at the intended temperature of use<sup>12b,27</sup> with a limiting percentage of crystallinity of around 20%, as seen by controlling the degree of cross-linking.

The influence of the observed morphologies was mirrored in the biodegradation study<sup>28</sup> with the same three representative particles of the  $AB_1$  series as above. Hydrolytic degradation tests were performed in vitro at pH 7.4 and a temperature of 37 °C with continuous stirring.<sup>29</sup> Samples were removed every 48 h over a time period of 240 h (10 days). The degradation of the particles was monitored by the change of the absolute molecular weight,<sup>30</sup> as determined through static light scattering illustrated in Figure 6 (see also Supporting Information). We observed a linear degradation profile for all investigated sizes as a result

**Table 3.** Nonaqueous Titration of Primary and Secondary Amines for Several  $AB_1$  Nanoparticle Samples

$AB_1$ nanoparticle size (nm)	primary amine wt %	secondary amine wt %
$58.1 \pm 6.2$	$0.008 \pm 0.001$	$0.031 \pm 0.001$
$255.7 \pm 26.9$	$0.025 \pm 0.001$	$0.100 \pm 0.002$
$425.1 \pm 44.6$	$0.055 \pm 0.002$	$0.200 \pm 0.002$

of the low crystallinity of the samples. The largest particle of  $725.1 \pm 94.3$  nm experienced the highest loss of molecular weight with 17.5% of total molecular mass remaining after 10 days. The smaller particle of  $115.6 \pm 12.5$  nm had a slightly higher degree of crystallinity of 20.6% and was degraded to 26.0% of the original molecular weight. An even smaller particle of  $30.7 \pm 2.2$  nm experienced an anticipated lower molecular weight loss, with 35% of remaining molecular mass of the particle. Future studies will include the investigation of particles with lower and even higher degrees of cross-linking densities and particles with integrated mixtures of different amounts of diamine-alkyl and diamine-ethoxy cross-linker to further extend the degradation profile to longer or shorter time frames, if needed.

The continuous increase in 2,2'-(ethylenedioxy)bis(ethylamine) cross-linker equivalents not only extends the particle size and maintains the increased hydrophilic behavior, but it also introduces additional amine functionalities that are created during the cross-linking event. The intermolecular cross-linking mechanism implements these valuable functionalities due to unreacted free amine units of the diamine cross-linking unit with the oxirane of the polyester backbone. In view of the further utilization of the amine groups in the final particle, we wanted to quantify the weight percent of primary and secondary amine groups using a nonaqueous salicylaldehyde titration, as reported in the literature.<sup>31</sup> The titration was completed by first reacting the primary amines with salicylaldehyde to form a salicylaldehyde-imine with several samples of  $AB_1$  particles. The unreacted secondary amines were titrated with standard perchloric acid in glacial acetic acid using bromocresol green indicator. After neutralization of the secondary amines, the salicylaldehyde-imines were titrated with the standard perchloric acid using congo red indicator. The results of the titrations (Table 3) show a consistent increase in the weight percents of both the primary and the secondary amines as the particle sizes increase, which is indicative of a controlled cross-linking process that leads to functionalized, well-defined, and amorphous particles.

In addition to amine functionalities, acetylene and keto groups have been successfully incorporated into the nanoparticles, as it is our goal to extend the availability of functional groups to provide the opportunity to tailor the physical and chemical properties of the nanoparticle. Utilizing the experimental conditions we established for the  $AB$  linear precursors, as previously discussed, linear copolymers  $ABC$ ,  $ABD$ , and  $ABCD$  were effectively transformed into nanoparticles via the facile cross-linking technique. With each copolymer, a series of nanoparticles were prepared in which the equivalents of amine were varied from 1 to 10 amines/epoxide entity within the polymer backbone, in line with the experiments we conducted with polymer  $AB_1$ . All three copolymers were found to respond in the same fashion as  $AB_1$  to the controlled chain cross-linking conditions to form distinct monodisperse nanoparticles (Table 4).

(27) Wang, Y. D.; Ameer, G. A.; Sheppard, B. J.; Langer, R. *Nat. Biotechnol.* **2002**, *20*, 602–606.

(28) Tserki, V.; Matzinos, P.; Pavlidou, E.; Panayiotou, C. *Polym. Degrad. Stab.* **2006**, *91*, 377–384.

(29) Giunchedi, P.; Conti, B.; Scalia, S.; Conte, U. *J. Controlled Release* **1998**, *56*, 53–62.

(30) Umare, S. S.; Chandure, A. S.; Pandey, R. A. *Polym. Degrad. Stab.* **2007**, *92*, 464–479.

(31) Shaffer, C. B.; Critchfield, F. H. *J. Pharm. Sci.* **1947**, *36*, 152.



**Table 4** Nanoparticle Size Dimensions (nm diameter by DLS) in Relation to Varying Amine Ratios

amine/1 epoxide	diameter (nm) AB <sub>1</sub> nanoparticles	diameter (nm) ABD nanoparticles	diameter (nm) ABC nanoparticles	diameter (nm) ABCD nanoparticles
1	30.7 ± 2.2	34.3 ± 3.2	21.4 ± 2.9	19.0 ± 1.8
2	58.1 ± 6.2	63.5 ± 7.7	41.7 ± 5.4	36.7 ± 2.2
3	82.6 ± 5.7	118.3 ± 13.6	114.9 ± 8.9	73.4 ± 5.3
4	115.6 ± 12.5	164.9 ± 17.2	148.3 ± 15.3	114.8 ± 9.2
5	255.7 ± 26.9	292.7 ± 32.2	186.1 ± 18.5	168.2 ± 16.5
6	342.2 ± 42.2	341.0 ± 32.4	253.9 ± 25.9	247.2 ± 14.5
8	425.1 ± 44.6	525.0 ± 55.4	472.1 ± 43.8	451.1 ± 20.4
10	725.1 ± 94.3	800.0 ± 135.0	675.0 ± 95.4	614.1 ± 56.2

Parallel to the formation of the AB<sub>1</sub> nanoparticles, a polynomial increase in the sizes of the ABC, ABD, and ABCD nanoparticles was observed as the amounts of diamine were increased (Figure 7, see also separate graphs of polynomial increase for each of the discussed particles in the Supporting Information).

We could conclude that the incorporated functionalities did not affect the particle formation and not participate in the cross-linking event, except for the designated oxirane unit. It also demonstrated that the formation of the particle is adaptable for a range of functionalized polyesters and is established by the amount of both of the adjustable cross-linking partners, the epoxide, and the diamine, respectively.

In order to advance the availability of functional groups, we sought to manipulate the quantities of each functional group incorporated into the particles. Therefore, we considered the effect of cross-linking two linear polymers together, such as ABC and ABD, in specific amounts, but with comparable epoxide percentages, to integrate particular selected quantities of acetylene and keto groups. The process began by cross-linking ABC with ABD in a 7/3 ratio with 4 equiv. of amine, which resulted in the formation of nanoparticles with a size dimension of 124.7 ± 6.7 nm, as observed by DLS. The size of these nanoparticles correlate to the sizes observed from cross-linking ABC, ABD, and ABCD independently with similar equivalents of amine, 164.9 ± 17.2, 148.3 ± 15.3, and 114.8 ± 9.2 nm respectively (Table 4). Characterization of the ABC-co-ABD particles by <sup>1</sup>H NMR confirmed the incorporation of both ABC and ABD in the nanoparticle in a ratio of 7/3, which further proves that the particles are formed by a controlled intermolecular cross-linking mechanism and provides yet another avenue for controlling the integration of functional groups in the nanoparticle.

With the presence of amine, acetylene, and keto functionalities in the nanoparticles, a wealth of chemical and physical modifications can be accomplished. We have begun to utilize these functional groups by employing the ketone carbonyls of ABD for reductive amination. We chose for the trial an ABD particle in 120-nm size dimension that was prepared with 3 equiv. of diamine cross-linker and 7% of epoxide incorporated in the linear precursor. The amine groups on the particle were first quenched with *N*-acetoxysuccinimide. For the next step, involving the reductive amination<sup>16</sup> of the keto groups, we selected *N*-Boc-ethylenediamine as a simple amine compound that allowed us to monitor a successful modification through the detection of the Boc resonance peak in <sup>1</sup>H NMR spectra which would not interfere with the other resonance peaks of the nanoparticle backbone. To guarantee maximum solubility of both components in the reaction mixture,

a 1:1 CH<sub>2</sub>Cl<sub>2</sub>/ MeOH mixture was chosen, with NaCNBH<sub>3</sub> as the reducing reagent.<sup>16a,32</sup> The amount of *N*-Boc-ethylenediamine was calculated to react with 40 keto groups. The functionalized nanoparticles were dialyzed with organic compatible dialysis tubing against 1:1 DCM/MeOH mixture to remove any of the small molecule reactants. The functionalized ABD particles were characterized by <sup>1</sup>H NMR that proved the attachment of the *N*-Boc-ethylenediamine linker to the polymer backbone of the nanoparticles with a corresponding resonance of the Boc methylene groups at 1.43 ppm which integrated to 37 groups of modified keto groups (see Supporting Information). Other post modification strategies including sequential attachments of bioconjugates and a dendritic transporter will be published in due course.

## Conclusions

In summary, a new direct method to provide distinct, functionalized polyester nanoparticles in any selected nanoscopic dimension from 8–700 nm has been presented. Ring-opening polymerization procedures provided linear copolymers of  $\delta$ -valerolactone with  $\alpha$ -allyl- $\delta$ -valerolactone,  $\alpha$ -propargyl- $\delta$ -valerolactone and 2-oxepane-1,5-dione. The allyl functionality was transformed into epoxide units as one of the critical cross-linking entities to facilitate the nanoparticle formation. The reaction of the epoxide units with diamine 2,2'-(ethylenedioxy)bis(ethylamine) led to the controlled preparation of nanoparticles, in which the size dimension depended on the amount of diamine present during the cross-linking process. Additionally, we showed that the nanoscopic dimensions could be controlled by the adjustment of incorporated epoxide groups per linear precursor. A higher percentage of epoxide gave larger particles with the same equivalents of amines present than smaller percentages. Furthermore, it was found that the cross-linking procedure is not influenced by other functionalities present in the linear polymers and demonstrates the universal nature of the developed procedure to gain access to functionalized polyester nanoparticles. With that said, not only identical, homogeneous linear polyesters can form nanoparticles with fixed amounts of functional units, but also the amount of functionalities such as keto-, alkyne, and amine groups per particle can be adjusted by mixing different linear polyesters with comparable epoxide percentages. In this way, a plethora of well-defined functionalized polyester nanoparticles can be prepared in different sizes and functionalities that are completely amorphous at the intended temperature of use. The first post-modification reactions have been employed with the attachment of *N*-Boc-ethylenediamine in a reductive amination reaction to prove the reactivity of keto groups in the effort to develop targeted drug delivery systems.

**Acknowledgment.** E.H. gratefully acknowledges Vanderbilt University for a startup fund and financial support from the NSF (CAREER) under Award No. CHE-0645737. The authors thank also Prof. Michael E. Mackay and Jon Kiel, Michigan State University, for their help in various aspects of the DLS measurements.

**Supporting Information Available:** Full experimental details as well as additional graphs, tables, and spectra of nanoparticle characterizations and modifications. This material is available free of charge via the Internet as <http://pubs.acs.org>.

JA711417H

- (32) (a) Yamamoto, Y.; Nagasaki, Y.; Kato, M.; Kataoka, K. *Colloids Surf., B* **1999**, *16*, 135–146. (b) Yamamoto, Y.; Nagasaki, Y.; Kato, Y.; Sugiyama, Y.; Kataoka, K. *J. Controlled Release* **2001**, *77*, 27–38.